

Flow and Concentration Pulses Increase Nitrate Removal Rates in a Woodchip Bioreactor

Nora Sauers

ASABE Member Number: 1060013

North Carolina State University, Raleigh, NC

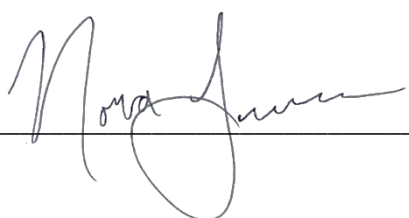
Graduation Date: May 2024

Advisor: Dr. François Birgand

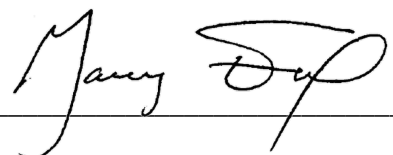
Department of Biological and Agricultural Engineering

The K.K. Barnes Student Paper Award Competition

Sponsored by the American Society of Agricultural and Biological Engineers

Student Signature:  _____

Date: May 15, 2023

Department Head Signature:  _____

Date: May 15, 2023

Project Selection

This project was an independent undergraduate research project conducted as part of the Biological and Agricultural Engineering Research and Educational Enhancement Projects (REEP) at NC State University. As a REEP scholar, the author was advised by a professor of her choice, Dr. François Birgand, to devise and execute a set of experiments through the course of the academic year. With Dr. Birgand's expertise in biogeochemical processes and denitrifying systems, the author investigated nitrate removal and carbon dynamics following drying-rewetting cycles in an aged woodchip bioreactor. In addition to leading experiments and sample collection, the student performed all data analysis in Microsoft Excel and R Studio and completed the present composition. The student did benefit from having the experimental and sampling platform ready to conduct the experiments reported.

Acknowledgements

I would like to acknowledge Dr. François Birgand for his involvement and dedication to the project by providing advice and assistance throughout the experiments. His expertise in the subject area of woodchip bioreactors was vital in the success of the study. I would also like to thank Adam Rok for his maintenance of the laboratory and for ensuring the experiments ran as intended. Without his ability to fix all unavoidable equipment failures during experiments, the project would not have been possible. Additionally, many thanks to the Environmental Analysis Laboratory at NC State University for water sample analysis to verify nitrate and dissolved organic carbon (DOC) concentrations.

Abstract

Woodchip bioreactors are extensively used to remove excess nitrate from subsurface drainage waters. These systems, as are all natural treatment systems existing at the edge-of-field, are subject to pulses of flow and nitrate concentrations following rainfall events. It is known that flow affects the mass of nitrate removed, as it controls the time that water may reside in these systems. However, it is unclear whether flow and concentration pulses affect removal rates, i.e., the mass of nitrate removed per unit volume of bioreactor per unit residence time. While denitrification may be enhanced as increased flow activates more pores where water would otherwise be stagnant, additional oxygen to the reactor may inhibit denitrification. Increased concentration is expected to increase concentration gradients at the microscale, hence increasing the overall removal rates. To determine the effects of increasing flow rate and concentration independently as well as in combination, a 4-month lab experiment was designed and performed on a 0.3 m by 0.3 m by 2.4 m-long lab bioreactor to obtain hourly nitrate and dissolved organic carbon (DOC) concentrations at twelve locations along the bioreactor filled with woodchips. The results demonstrate that the removal rates during pulses were up to four times greater than the removal rates during baseline conditions. These results are important because they demonstrate a potential to revolutionize the design, operation, and management of bioreactors and other edge-of-field subsurface treatment systems in the field.

Introduction

Nitrate is the stable inorganic form of reactive nitrogen in aerobic conditions. The doubling of nitrogen fixation from atmospheric N_2 by anthropogenic activities (e.g., industrial production of fertilizer, fixation by agricultural crops, and combustion of fossil fuels; Fowler et al., 2013) has rendered nitrate to be the preponderant reactive nitrogen form in streams and groundwater. Excess nitrate can result in environmental problems such as eutrophication and harmful algae blooms in coastal waters (e.g., National Research Council, 2000; Anderson et al., 2002). Natural systems such as wetlands, existing or installed near nitrate sources such as artificial drainage water, remove nitrate through denitrification which requires anoxic conditions, the availability of nitrate as the electron acceptor, and an abundance of organic material to act as the electron donor (Van Cleemput et al., 2007).

Engineered denitrifying bioreactors installed at the edge-of-field utilize the same basic processes as wetlands; in saturated, anaerobic conditions, a carbon source such as woodchips serves as the energy source or electron donor while nitrate provides the electron acceptor, allowing denitrification to occur and reduce nitrate into nitrogen gases that escape the aquatic environment (Addy et al., 2016). Woodchips are often used as a carbon source in denitrifying bioreactors as a cost-efficient, high carbon-to-nitrogen-ratio material with slow carbon depletion (Healy et al., 2012). Woodchip bioreactors are used in numerous applications such as treatment of water from livestock farms, crop fields, aquaculture and hydroponics systems, as well as urban and stormwater applications (Maxwell et al., 2019a).

Research has shown that denitrification rates within woodchip bioreactors are variable and can be affected by a variety of factors within the system including nitrate concentration, water temperature, hydraulic retention time, wood chip age, and drying-rewetting cycles (Addy et al., 2016; David et al., 2016; Maxwell et al., 2019a, 2019b). In most agricultural settings, nitrate is available in excess, and denitrification is generally limited by accessible labile carbon within the bioreactor. When nitrate is present in low enough concentrations to limit denitrification, increasing the amount of nitrate increases nitrate removal rates (Schipper et al., 2010). Woodchip bioreactors demonstrate highest removal rates when nitrate concentrations are above 30 mg N/L and show lowest removal rates with concentrations

below 10 mg N/L (Addy et al., 2016). Nitrate removal rates in bioreactors have been shown to decrease with lower water temperatures (Volokita et al., 1996) with temperature acting as a particularly limiting factor in older woodchip bioreactors (Addy et al., 2016; David et al. 2016; Maxwell et al., 2020).

Bioreactors require sufficient time for nitrate removal with decreased nitrate removal rates observed when retention times are less than 6 hours (Addy et al., 2016).

Denitrifying woodchip bioreactors have demonstrated the ability for long-term nitrate removal (Robertson et al., 2000). However, there have been mixed results surrounding the effects of woodchip aging on nitrate removal rates. While denitrification rates in woodchip bioreactors often remain stable after multiple years of use, there may be a significant decrease in nitrate removal efficiency after the first year of operation with up to 50% of reactivity lost (Robertson, 2010; Addy et al. 2016). Increasing the surface area available for denitrification by manually breaking down the carbon substrate has inconsistent effects on nitrate removal in bioreactors (Greenan et al., 2006). This raises the question as to how denitrification rates change within aged bioreactors as woodchips are broken down into smaller pieces. A possibility is that denitrification is not limited to the outer surface area, as aged wood particles displaying darkened rims indicate denitrification zones that penetrate the solid material (Robertson et al., 2000).

Drying-rewetting (DRW) cycles have been shown to enhance denitrification rates in woodchip bioreactors and offer the possibility to offset decreased nitrate removal in aged bioreactors. DRW cycles create intermittent aerobic conditions when water is drained from the bioreactor for several hours, leaving the woodchips unsaturated but still moist, followed by re-saturation of the bioreactor. The period following rewetting is accompanied with an increase in greater total carbon (TC) and dissolved organic carbon (DOC), fueling denitrification by providing more carbon (Maxwell et al., 2019a; Maxwell et al., 2019b; McGuire et al., 2021) and likely labile carbon of higher quality for microbial activity (Zarnetske et al., 2011), as also observed during DRW cycles in normally unsaturated soils (Miller et al., 2005). Increased duration of the unsaturated period may increase denitrification rates linearly with drying periods of up to 48 hours (Maxwell et al., 2019a, 2019b; McGuire et al., 2021) with these increased rates continuing up to four days after re-saturation (McGuire et al., 2021).

Finally, the impact of flow rates on denitrification is unclear. Increased nitrate reduction has been observed with high retention times compared to low retention times, although the most efficient flow rate for bioreactors is unclear (Chun et al., 2009). A laboratory study using small bioreactors to simulate denitrification from tile drained fields in Iowa concluded that $\text{NO}_3\text{-N}$ removal efficiency decreased with increasing flow rate (Greenan et al., 2009).

This review of the literature reveals that limited research has been done on the impacts of the pulsed nature of flow and pollutant loads in watersheds, although this is paramount in the functioning of these systems. Following rainfall events, natural and man-made subsurface filter systems at the edge-of-field (e.g., riparian zones, saturated buffers, woodchip bioreactors) undergo pulses of flow and concentrations. In most climates suitable for agriculture, rainfall events are relatively rare: 30-50% of watershed annual flow volumes transit through these systems in less than 10% of the time (e.g., Birgand et al., 2011). For the edge-of-field subsurface filter systems to play their surmised nitrate removal role in the annual nitrogen budget at the watershed scale (e.g., Burt et al., 2010), *the volumetric removal rates of the soil/substrate must dramatically increase during flow pulses* to compensate for the rarity and the short hydraulic residence time in these systems during these rare events. This has yet to be shown.

As a result, a research question was proposed to determine whether volumetric nitrate removal rates in edge-of-field subsurface treatment systems increase during flow and concentration pulses, and if so, to what extent. We hypothesized that denitrification should be enhanced during these pulses, as increased flow may activate additional pores where water would otherwise remain stagnant, corresponding to increased DOC production. Additionally, the increased concentration is expected to amplify concentration gradients at the microscale, thereby increasing overall removal rates.

To date, this question has remained unanswered due to the lack of suitable monitoring techniques and instruments capable of accurately capturing the fate of nitrate during these infrequent yet significant events. While this question pertains to all edge-of-field subsurface systems, a promising initial approach is to investigate the impact of flow and concentration pulses on volumetric removal rates in a woodchip bioreactor.

To address this question, a 4-month laboratory study was conducted in a horizontal woodchip bioreactor with a constant saturated volume. High-frequency monitoring was conducted along the length of the bioreactor to assess the effects of flow and nitrate concentration pulses, as well as their combined effect, on nitrate and dissolved organic carbon (DOC) concentrations and volumetric removal rates.

Materials and Methods

Experimental Design

To determine the effects of concentration and flow pulses on nitrate volumetric removal rates, a horizontal woodchip bioreactor system receiving nitrated water was used. The bioreactor consisted of an open-top plexiglass tank with a length, width, and depth of 2.4 m by 0.3 m by 0.3 m containing 5-yr aged woodchips with an effective volume of 148.2 L and a drainable porosity of 84 L or 57%.

The experimental setup is illustrated in Figure 1. Two 1135-L and one 150-L tank were utilized for dosing tap water with KNO_3 and as sources to the bioreactor. One large tank was reserved for dosing and was constantly aerated with an aquarium pump to degas chlorine from the tap water and supplied the two other tanks used as source tanks for the bioreactor. The smaller tank was used during the concentration pulse experiments. During experiments, water was pumped from the source tanks into an overflow reservoir to provide a constant head, and the flow rate in the bioreactor was adjusted using a valve. The water level in the bioreactor was adjusted with a control structure at the outlet. At the end of each weekly experiment, the control structure was lowered to drain water from the bioreactor. At the beginning of an experiment, the downstream control structure was raised, and the bioreactor was filled directly from the pump within 10 min. The water level was maintained at $22.5 \text{ cm} \pm 2 \text{ mm}$ above datum for all experiments (flux surface area of 0.069 m^2). The bioreactor was fed via the overflow/valve system at flow rates varying between 4 and 18 mL/s (water fluxes of 5 to 20 m/d). Flow rates were measured manually at the outlet several times a day using a graduated cylinder and a stopwatch and automatically using a rain gauge tipping bucket system from Texas Electronics Inc. and recorded using a Hobo® pendant event logger from Onset® during low flow conditions.

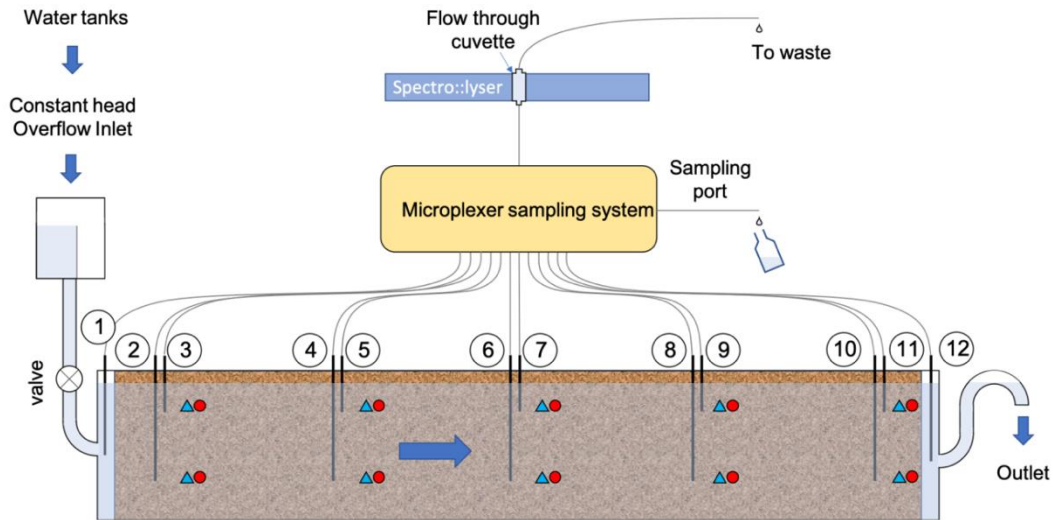


Figure 1: Layout of the experimental setup. KNO_3 solutions were prepared in water tanks using tap water aerated with an aquarium pump to remove chlorine. Every 4-6 minutes, water was sequentially sampled upstream, downstream, and along the flow path (at two different depths; 10 and 20 cm from bioreactor bottom) from each of the 12 sampling ports using a 12-valve Microplexer automatic sampling system (MPS) to a flow-through cuvette installed on the Spectro::lyser™ from S::CAN™. Time resolution on each port was ~50 min. Dissolved oxygen concentrations (blue triangles) and temperatures (red circles) were measured at 10 points just downstream of sampling ports 2-11 every 2 minutes.

Five series of three experiments were conducted. Each experiment consisted of three- to five-day flow periods, beginning after the woodchips had been exposed to aerobic conditions for 40-48 hours following the previous experiment, providing the ‘drying’ period of DRW cycles to stimulate denitrification. The results of one five-day period from each of the five series were chosen to be analyzed. The selected periods were most representative of the experimental conditions described, e.g., constant flow or constant NO_3^- inlet concentration with no system or equipment failures.

Flow and concentration pulses were implemented as step functions of low and high values. The details of the targeted flow and concentration pulse values are summarized in Table 1. The first experiment determined the baseline conditions of the woodchip bioreactor with a constant flow of approximately 4.5 mL/sec (corresponding to a flux of 5.67 m/d and a theoretical hydraulic residence time

of approximately 5.2 hours) and constant concentration of 5 mg N/L of NO_3^- . The second experiment evaluated the effect of pulsed, increased flow rates while maintaining a constant concentration of 5 mg N/L of NO_3^- . The baseline flowrate was approximately 5 mL/sec and elevated flow pulses of 10-15 mL/sec were applied to the bioreactor each day for several hours. The third experiment tested the impact of elevated concentration pulses. A constant flow of 4-6 mL/sec was maintained with a baseline concentration of 5 mg N/L and high concentration pulses of 10 mg N/L applied for 8 hours daily. The fourth and fifth experiments examined the effects of applying combined high nitrate concentration and high flow rate pulses to the system. The fourth experiment maintained baseline low flow and low concentration conditions with short, 3-hour pulses of high flow and high concentration daily. The fifth experiment maintained long pulses of high flow and high concentration for 14-16 hours with baseline low flow and low concentration conditions for 8-10 hours. Low flow conditions and high flow conditions were performed at flow rates of 5 mL/sec and 15 mL/sec, respectively. Low concentration conditions and high concentration conditions consisted of nitrate-dosed water at 5 mg N/L and 10 mg N/L, respectively.

Sampling System

To capture the impacts of flow and concentration pulses, we used a high-frequency water quality sensor coupled with a multiplexed sampling (MPS) system. The sensor was a Spectro::lyser™ spectrophotometer from S::CAN™ able to measure nitrate and DOC concentration at the minute scale. The MPS (Maxwell et al., 2018) sequentially pumped water from 12 ports along the flow path to the spectrophotometer fitted with a flow-through quartz cuvette (1-Q-10/SBTX2-8/10X20 from Starnacell®) every 4-6 minutes (time varied among experiments) such that approximately 50 min data was acquired for each port. To minimize sample volume, 0.9 mm inside diameter Teflon® tubing was used for a total of approximately 25 ml per sample. A sampling sequence started at the outlet (Port 12) and ended at the inlet (Port 1) to minimize the impact of sampling. Each port was fitted with a fine mesh screen (plankton net) effectively filtering sizable particulate carbon out of the tubing system.

Table 1: Summary of the targeted flow and nitrate concentration values for the five experiments analyzed. The water fluxes through the bioreactor (flow rate divided by the cross-sectional area), and the theoretical hydraulic residence time (HRT - drainable porosity divided by the flow rate) are reported for comparison purposes.

Experiments	Low Flow rate (mL/sec) <i>Flux (m/d)</i> Theoretical HRT (h)	High Flow rate (mL/sec) <i>Flux (m/d)</i> Theoretical HRT (h)	Low nitrate concentration (mg N/L)	High nitrate concentration (mg N/L)
1 - Baseline conditions	4.5 5.67 5.2	-	5	-
2 - Flow pulses	5 6.30 4.7	10 to 15 12.6 to 18.9 2.3 to 1.6	5	-
3 - Concentration pulses	5 6.30 4.7	-	5	10
4 - Flow + Concentration short pulses	5 6.30 4.7	10 12.6 2.3	5	10
5 - Flow + Concentration long pulses	5 6.30 4.7	10 12.6 2.3	5	10

The twelve water sampling ports were placed in both the inlet and outlet in addition to five inner pairs of sampling ports positioned approximately 50 cm apart (Figure 1). Each pair consisted of a shallow port and deep port at depths of 10 cm and 20 cm from the surface, respectively. To monitor anoxic and ambient conditions within the bioreactor, ten PreSense™ Oxy-10 SMA oxygen and temperature sensor probes were placed adjacent to the water sampling ports (Figure 1).

Water samples were collected by hand in combusted amber bottles twice per week for each experiment at the discharge of the cuvette following measurements by the Spectro::lyser™ directly from dedicated port on the MPS during purging. Samples were acidified with sulfuric acid and refrigerated after collection. Twelve samples from each experiment were analyzed at the Environmental Analysis Laboratory (EAL) at NC State University for calibration of the Spectro::lyser™ concentrations. Nitrate concentrations were analyzed using the EPA Method 410.4 with an Autoanalyzer System. DOC

concentrations were analyzed using Standard Methods 5310 B with a Teledyne Tekmar Apollo 9000 combustion TOC analyzer.

Data Analysis

To establish concentration time series for each sampling port, the date and time were used as a unique identifier, and each sampling port (1-12) was allocated to nitrate and DOC concentrations of the spectrophotometer concentration time series in RStudio (R Studio Team, 2020). To calibrate the nitrate and DOC concentrations, measurements collected from the spectrophotometer were compared to the samples analyzed in the EAL for each experiment. For DOC, concentrations were calculated from the instrument absorbance spectra using a partial least square regression (PLSR) established between laboratory values and absorbances measured on the manual samples following procedures established by Etheridge et al. (2014). For nitrate, concentrations were calculated from a standard linear regression established between concentrations calculated from S::CAN and those from the laboratory. The R-squared values for the regressions varied between 0.97 and 1.00.

Each sampling port time series had approximately 50-min resolution, which were all shifted by approximately 5 min corresponding to the spectrophotometer measurement resolution. For harmonization purposes to calculate loads, 5-min synchronous concentration and flow time series were created using linear interpolation between measured points. Instantaneous and cumulated nitrate and DOC loads were calculated as follows:

$$l_i = C_i Q_i \quad (1)$$

$$L(T) = \sum_{i=0}^{i=N} \frac{C_i Q_i + C_{i+1} Q_{i+1}}{2} \cdot \Delta t \quad (2)$$

with l_i and $L(T)$, respectively, the instantaneous and cumulative loads over the experimental time T with Δt the time series resolution, $N = \frac{T}{\Delta t}$, C_i and Q_i , instantaneous concentrations and flow rates.

Total volumetric nitrate removal ($R_v(T)$) and volumetric DOC production ($P_v(T)$), over the whole experimental times T , were calculated by subtracting the cumulated nitrate ($L_{(N)}(T)$) and DOC

$(L_{(C)}(T))$ loads at the inlet (L_{in}) and outlet (L_{out}), divided by the volume of saturated woodchip in the bioreactor (V) and by T to finally obtain values expressed in $\text{g/m}^3/\text{day}$:

$$R_v(T) = \frac{(L_{(N)in}(T) - L_{(N)out}(T))}{V \times T} \quad (3)$$

$$P_v(T) = \frac{(L_{(C)out}(T) - L_{(C)in}(T))}{V \times T} \quad (4)$$

The relationship between R_v and P_v was investigated using the “cor” function in R to determine the Pearson correlation coefficient between the two variables (RStudio, 2020).

When pulses are applied to the system, an integrative variable such as $R_v(T)$ was not indicative of the effects of the treatment within the pulses compared to the baseline conditions of the experiment outside the pulses. Therefore, two methods were developed to quantify the nitrate removal rates during pulse and baseline conditions and account for artificial removal rates. The percentage increase was calculated for each method from the baseline conditions to the pulse conditions of each experiment.

Method 1 was devised to highlight the effect of pulses on the volumetric removal rates compared to baseline conditions. Apparent instantaneous nitrate volumetric removal rates R_{vi} and instantaneous carbon volumetric production rates P_{vi} (i for instantaneous) were calculated as:

$$R_{vi} = \frac{(l_{i(N)in} - l_{i(N)out})}{V \times T} \quad (5)$$

$$P_{vi} = \frac{(l_{i(C)out} - l_{i(C)in})}{V \times T} \quad (6)$$

where $l_{i(N)}$ and $l_{i(C)}$ are the instantaneous, respectively, nitrate and DOC loads at the inlet (l_{in}) and outlet (l_{out}). The formulae for R_{vi} and P_{vi} assume that treatment is instantaneous, which it is not. The time series of R_{vi} thus shows artificial peaks and troughs at the transition between baseline and pulse conditions as shown in Figure 2, but also relatively stable values during the pulses.

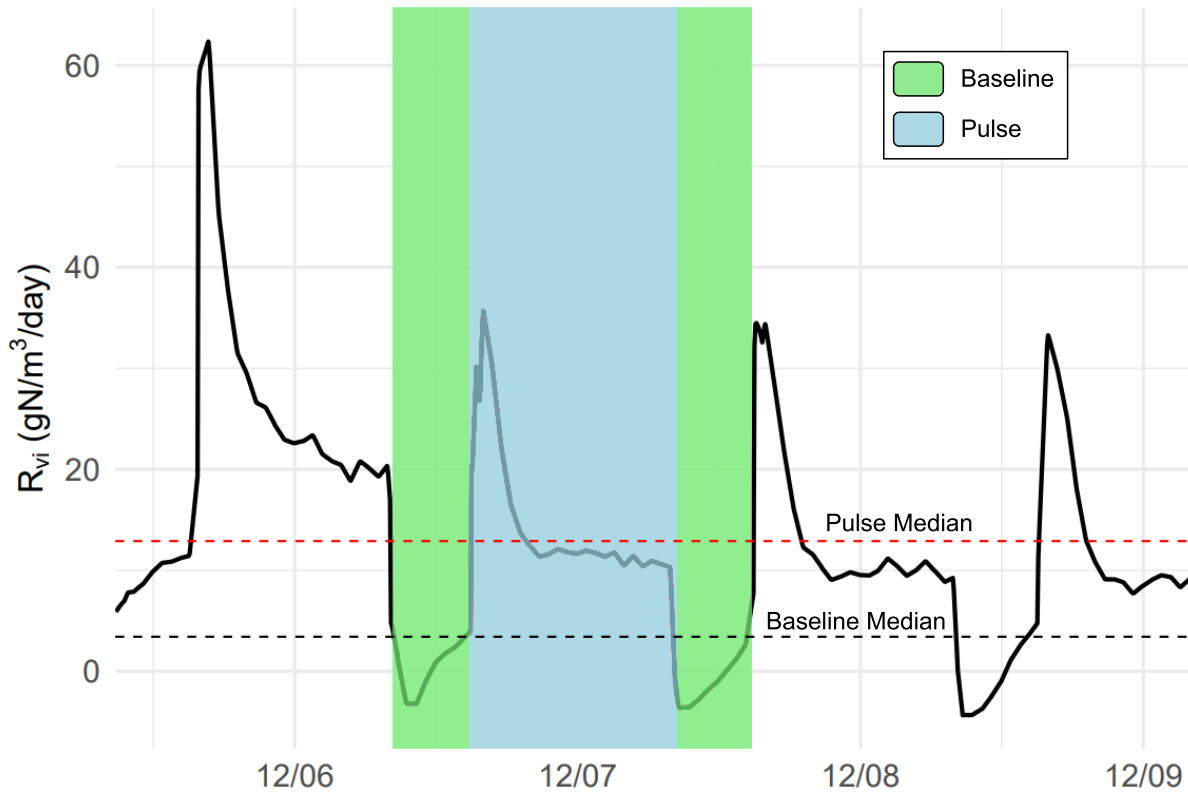


Figure 2: A comparison of volumetric nitrate removal rate during baseline and pulse conditions during each experiment as calculated by Method 1 and Method 2. Method 1 calculated removal rates using median values based on pulses in the volumetric nitrate removal. Method 2 calculated removal rates by scaling total mass removed for baseline periods and pulse periods during each experiment.

In Method 1 (Figure 2), the median R_{vi} within each pulse and each baseline period for the separate experiments was calculated by identifying the beginning and end of each pulse as demonstrated by the time series of R_{vi} (Figure 2). Artificial negative values were removed, and the medians of each pulse and baseline period were then averaged to determine an overall pulse R_{vp1} (p for pulse and 1 for method 1) and baseline R_{vb1} (b for baseline and 1 for method 1) for each experiment. The average was taken over the median to account for the true variation between pulses, as seen in Figure 2. As the first experiment included exclusively baseline conditions, the median of all R_{vi} values throughout the experiment was calculated to determine the overall R_{vi} .

In Method 2, we assumed that the overall cumulative $R_v(T)$ calculated using equation 3 was also the weighted summation of the average baseline and pulse R_{vi} , weighted by their relative occurrence

(equation 8). Depending on the pulse applied, i.e., flow or concentration, the beginning and end of the pulses were determined based on the corresponding time series to calculate the duration of pulse and baseline conditions. The median baseline R_{vb2} (b for baseline and 2 for Method 2) was used for baseline conditions except for the long pulses experiment, which exhibited short baseline conditions with artificial negative values implying that the system did not have time to stabilize between pulses; instead, the average of the final values for R_{vi} before each pulse was considered as most representative of stable baseline conditions (equation 7). Pulse R_{vp} for each experiment was determined from the difference between total mass removed and baseline mass removed, scaled by the duration of the pulse period (equation 8):

$$R_{vb2} = \text{median}(R_{vbi}) | \max(R_{vbi}) \quad (7)$$

$$R_{vp2} = \frac{R_v(T) \times T - R_{vb2} \times T_b}{T_p} \quad (8)$$

where T_b and T_p are the durations of the baseline and pulse conditions such that $T = T_b + T_p$.

Results

For clarity purposes, results from the inlet and outlet sampling ports only are presented in this manuscript. Typical data obtained are illustrated in Figure 3 below corresponding to experiment 5 (Table 1) with long pulses of flow and concentration. Water temperature in the bioreactor varied between 20.5°C and 23.0°C. Dissolved oxygen results (data not shown) suggest that, even during flow pulses, there was no measurable dissolved oxygen in porewater 30 cm from the inlet suggesting anaerobic conditions in >90% of the bioreactor volume.

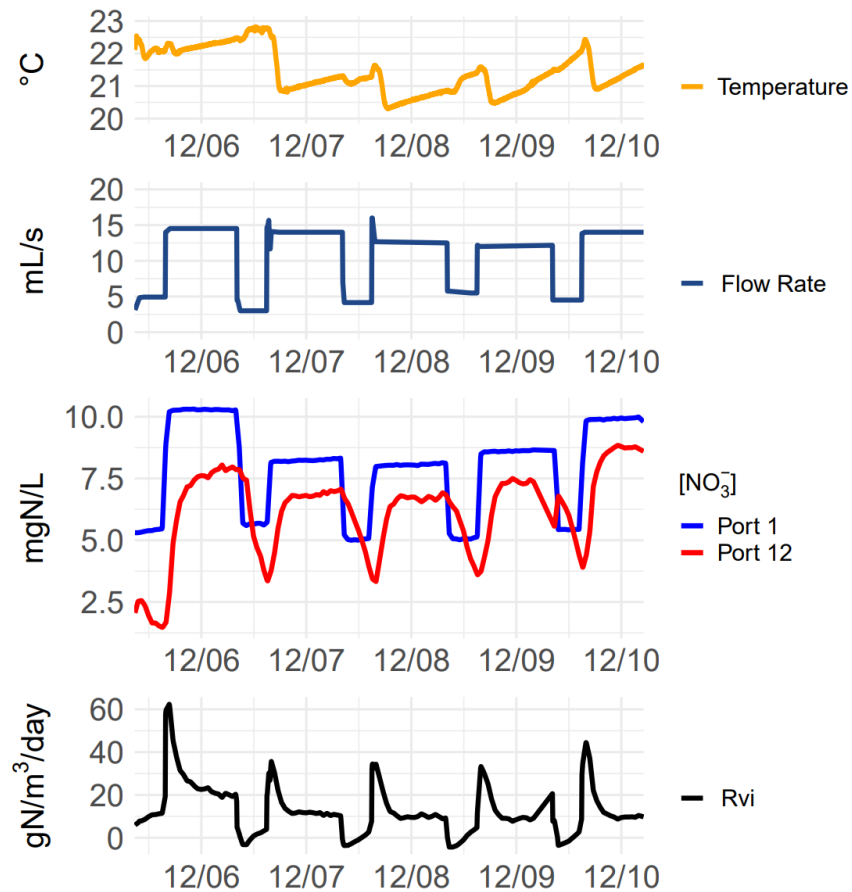


Figure 3: Bioreactor temperature, flowrate, inlet and outlet concentration, and volumetric nitrate removal rate during long pulses of increased concentration and flow.

Sudden temperature decreases corresponded to the change of source tanks, which for this experiment was the large tank recently dosed using lower temperature tap water. Figure 3 illustrates the step pulses of flow and concentration at the inlet. There was a very small delay (less than 15 min; data not shown) in flow adjustment at the outlet, and inlet and outlet flows were considered equal in the analysis. The steps of the inlet concentration pulses were not as ‘square’ at those of flow, as there was some mixing between the consecutive solutions in the overflow box and the piping upstream the inlet. The nitrate chemograph at the outlet was always lower than at the inlet, and it exhibited a lag and attenuation of the step function (Figure 3). Because of the lag, the apparent instantaneous R_{vi} showed artificial peaks after the beginning of a pulse and artificial troughs after the end of the pulses (Figure 2 and 3).

Table 2: Volumetric removal rates expressed in g/m³/day between baseline conditions R_{vb} and pulses R_{vp} calculated using two different methods, and the differences between the two ΔR_{vi} in absolute and percentage values.

Experiment	Method 1			Method 2		
	R_{vb1}	R_{vp1}	ΔR_{vi1} (%)	R_{vb2}	R_{vp2}	ΔR_{vi2} (%)
1 – No pulse low flow	12.49	-	-	13.31	-	-
2 –Flow pulses	13.35	13.24	-0.11 -1%	13.35	14.24	+0.89 +7%
3 – Nitrate pulses	10.35	23.68	+13.33 +127%	10.34	19.48	+9.14 +88%
4 – Short C+Q pulses	9.72	39.83	+30.11 +289%	9.79	25.29	+15.5 +158%
5 – Long C+Q pulses	3.83	13.03	+9.2 +140%	5.72	17.21	+11.49 +201%

All experiments demonstrated similar (flow pulses – experiment 2) or in most cases increased apparent removal rates (R_{vi}) during pulse conditions compared to baseline conditions. The removal rates increased with the highest enhancement evident in the short pulses of high flow and high concentrations, followed by long pulses of combined flow and concentrations, followed by concentration pulses alone (Table 2 and Figure 4). Short, high concentration and flow pulse conditions resulted in the greatest ΔR_{vi} , with increases of R_{vp} compared to R_{vb} of +310% (4.1 times the baseline value) and +158% (3.0 times the baseline value) as determined by Method 1 and Method 2, respectively (Table 2). The fifth experiment of long pulses of increased concentration and flow also experienced an increase in R_{vi} , although of lower amplitude (Figure 4). The nitrate pulses alone also largely increased the R_{vi} roughly by a factor of 2 (Table 2 and Figure 4).

The nitrate removal rates during baseline conditions were observed to diminish over the course of the study (Figure 4), excluding the experiment of high flow pulses. The percent decrease in volumetric removal rate in baseline conditions for Method 1 and Method 2 was -17% and -22% for the high concentration experiment, -22% and -26% for the short pulses experiment, and -69% and -57% for the long pulses experiment.

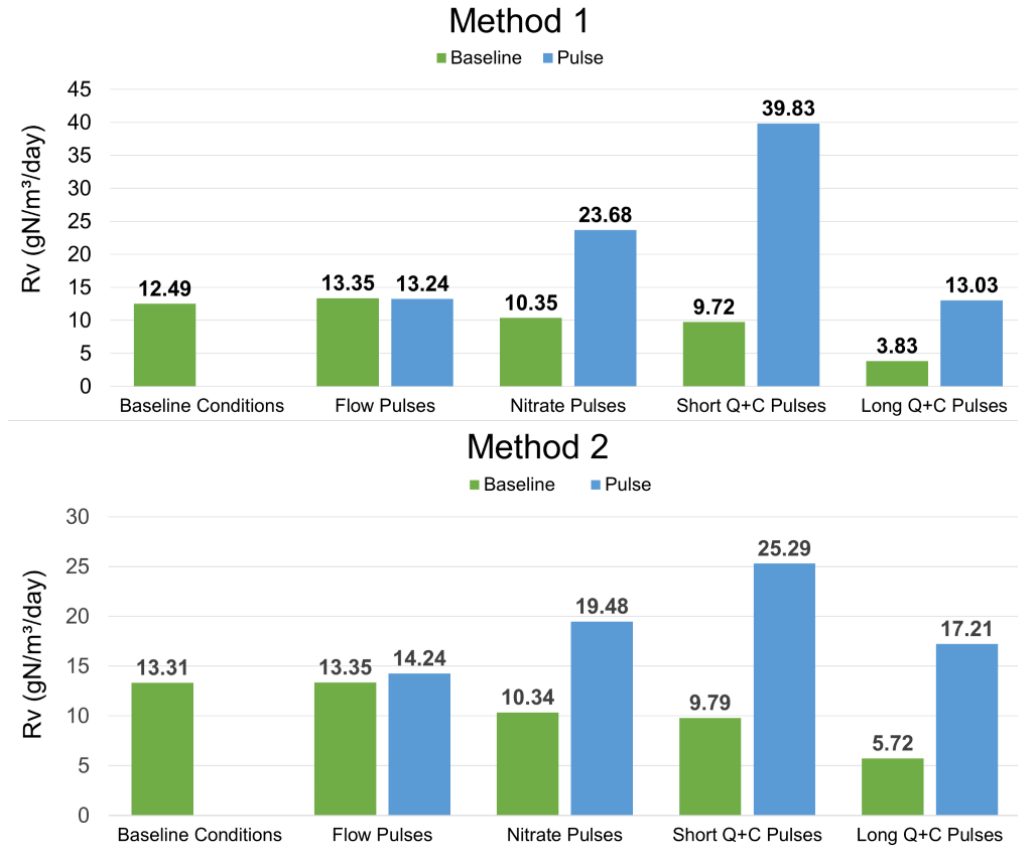


Figure 4: A comparison of volumetric nitrate removal rate during baseline and pulse conditions experiment as calculated by Method 1 and Method 2. Method 1 calculated removal rates using median values of the apparent instantaneous rates R_{vi} during baseline and pulsed conditions. Method 2 calculated removal rates by scaling total mass removed $R_v(T)$ for baseline R_{vb2} and pulse R_{vp2} periods during each experiment.

To unveil the possible mechanisms for the enhancement of the volumetric removal rates, the apparent volumetric nitrate removal rates (R_{vi}) and the volumetric DOC production rates (P_{vi}) were compared by calculating the Pearson correlation. At the beginning of all experiments, the DOC concentrations were highest, yielding the highest P_{vi} (Figure). The P_{vi} exhibited the same artificial peak as those of R_{vi} at the beginning of pulses, but not the corresponding troughs at the end of the pulses.

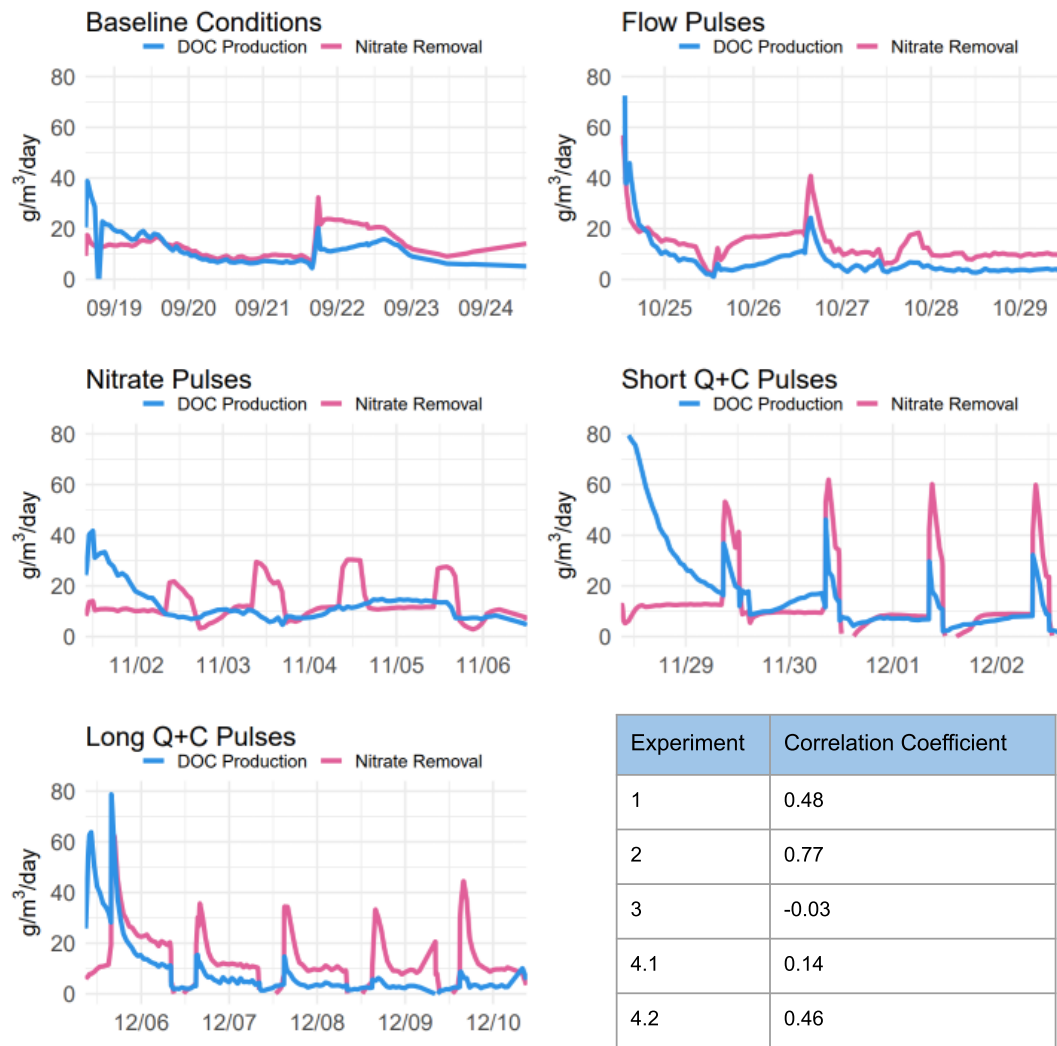


Figure 5: The correlation between volumetric nitrate removal and DOC production rates for each experiment as determined by the Pearson Correlation Coefficient. The short pulses experiment had the highest correlation of 0.77.

During all but the nitrate pulse experiment, the Pearson correlation coefficient demonstrated a possible correlation between R_{vi} and P_{vi} (Figure 5). During the standard baseline conditions of the first experiment, R_{vi} and P_{vi} have a slight positive correlation of 0.48 (Figure 5). The correlation between R_{vi} and P_{vi} increased to 0.77 during the flow pulse experiment. conditions in the second experiment with no positive correlation during high nitrate concentration pulses during the third experiment (Figure 5). Based on the Pearson correlation coefficient, there was not a strong correlation between R_v and P_v during the combined increased flow and increased concentration pulse conditions (Figure 5). Despite low correlation

coefficients, the combined increased flow and concentration pulses share distinct patterns in the time series with peaks of P_v occurring with peaks of R_v (Figure 5). In the combined short pulse experiment, there appears to be a strong correlation between the pulses of R_v and P_v (Figure 5). The correlation coefficient appears to be diminished by the lack of correlation at the beginning of the experiment; the initial elevated P_v is not represented in the R_v graph (Figure 5). A similar pattern is recognized in the long pulses; however, the peaks in P_v are less prominent (Figure 5). Correlation between DOC production and nitrate removal in the combined long pulses may be limited by differences in magnitude of the peaks.

An increase in DOC production rate is evident at the beginning of each experiment represented by a peak in the time series graph following the drying-rewetting cycles (Figure 5). There is a corresponding increase in nitrate removal rate at the beginning of the increased flow experiment with the highest correlation between R_v and P_v , which is not observed in the other experiments (Figure 5).

Discussion

The results provide evidence that pulses of increased flow and nitrate concentration, independently and in combination, are accompanied by a large increase in nitrate volumetric removal rates in edge-of-field subsurface treatment systems, and in our case in an aged woodchip bioreactor. The two methods developed to quantify volumetric removal rates yield very similar results for baseline rates R_{vb} , and pulse rates R_{vp} for all but the short combined pulses (experiment 4) where the first method yielded much higher pulse values. This probably is an artefact of the method because during short pulses the system does not reach equilibrium and some of the peak R_{vi} are artificial. Method 2, which minimizes these artefacts, still suggests that short pulses had the most relative effect on R_v , followed by long combined pulses of flow and concentration, and nitrate concentration pulses. The effect of increased flow offers the least stimulation of removal rates, possibly because denitrification was predominantly nitrate limited at an inlet concentration of 5 mg N/L, as nitrate pulses suggest.

The high correlation between nitrate removal rates R_v and DOC P_v during flow pulses, suggests, however, that flow pulses rendered DOC more available and/or removed toxic phenolic substances, which in the end benefitted anaerobic respiration (Fenner et al., 2005, 2011; Saraswati et al., 2016). The lack of correlation for the nitrate pulses suggest that denitrification was clearly nitrate limited with inlet concentrations at 5 mg N/L. Combining pulses of nitrate and flow appears to provide, especially for the short pulses, more than the addition of the benefits of the nitrate and flow pulses taken separately.

These results provide, for the first time to our knowledge, firm evidence that the metabolic rates in edge-of-field subsurface flow treatment systems increase during rainfall events which carry a large proportion of flow volume and nitrate loads to streams and rivers. If volumetric removal rates stayed constant regardless of flow, the significance of edge-of-field subsurface treatment would diminish proportionally to flow increase and in fact flow volumes. Our results show that with flow multiplied by 3 and nitrate concentrations multiplied by 2, i.e., the loads multiplied by 6, the volumetric rates were roughly multiplied by 3, suggesting that flow pulses may be accompanied with metabolic rates pulses or 'hot moments' (McClain et al., 2003).

Denitrification activity might have been stimulated in our woodchip bioreactor due to weekly 40-48 hour aerobic conditions and relatively high temperatures compared to a field bioreactor. However, drying-rewetting cycles are expected to naturally occur in other systems such as saturated buffers and riparian zones. Using 5 mg N/L for baseline inlet concentration might have created nitrate limitation, but these concentration levels are regularly observed in riparian systems (Jaynes and Isenhardt, 2019; Burt et al., 2010), although less so in woodchip bioreactors (Addy et al., 2016). Acquiring flow and concentration data at the appropriate resolution in time were decisive in obtaining our results. However, these results must be confirmed in additional laboratory and field settings to confirm and further quantify the respiratory process stimulations during the essential, although rare, flow events.

Conclusion

Pulses of increased flow and nitrate concentration enhanced the volumetric nitrate removal rates in a nitrate-limited, aged woodchip bioreactor following drying-rewetting cycles. The most effective treatment for enhancing volumetric nitrate removal rate proved to be short duration pulses of increased flow and increased nitrate concentration. These pulses enhanced the removal rates of the system by up to 2-4 times from the standard baseline conditions. It is hypothesized that pulses of high flow activated additional pores in the woodchip bioreactor for increased denitrification, while nitrate pulses decreased nitrate limitation of denitrification. The combined effect of increased activation of pores with high nitrate concentration enhanced removal of nitrate more than the addition of the pulses of flow and nitrate taken separately. Although they need to be confirmed, these results provide, for the first time, firm evidence that the metabolic rates in edge-of-field subsurface flow treatment systems increase during rainfall events which carry a large proportion of flow volume and nitrate loads to streams and rivers.

References

- Addy, K., Gold, A. J., Christianson, L. E., David, M. B., Schipper, L. A., & Ratigan, N. A. (2016). Denitrifying Bioreactors for Nitrate Removal: A Meta-Analysis. *Journal of Environmental Quality*, 45(3), 873–881. <https://doi.org/10.2134/jeq2015.07.0399>
- Anderson, D. M., Glibert, P. M., & Burkholder, J. M. (2002). Harmful Algal Blooms and Eutrophication: Nutrient Sources, Composition, and Consequences. *Estuaries*, 25(4), 704–726.
- Birgand, F., Faucheux, C., Gruau, G., Moatar, F., & Meybeck, M. (2011). Uncertainties in assessing annual nitrate loads and concentration indicators: Part 2. Deriving sampling frequency charts in Brittany, France. *Transactions of the ASABE*, 54, 93-104. <https://doi.org/10.13031/2013.36263>
- Burt, T. P., Pinay, G., & Sabater, S. (2010). *Riparian Zone Hydrology and Biogeochemistry*. International Association of Hydrological Sciences.

- Chun, J. A., Cooke, R. A., Eheart, J. W., & Kang, M. S. (2009). Estimation of flow and transport parameters for woodchip-based bioreactors: I. laboratory-scale bioreactor. *Biosystems Engineering*, 104(3), 384–395. <https://doi.org/10.1016/j.biosystemseng.2009.06.021>
- David, M. B., Gentry, L. E., Cooke, R. A., & Herbstritt, S. M. (2016). Temperature and Substrate Control Woodchip Bioreactor Performance in Reducing Tile Nitrate Loads in East-Central Illinois. *Journal of Environmental Quality*, 45(3), 822–829. <https://doi.org/10.2134/jeq2015.06.0296>
- Etheridge, J. R., Birgand, F., Osborne, J. A., Osburn, C. L., Burchell, M. R., & Irving, J. (2014). Using in situ ultraviolet-visual spectroscopy to measure nitrogen, carbon, phosphorus, and suspended solids concentrations at a high frequency in a brackish tidal marsh. *Limnology and Oceanography: Methods*, 12, 10–22. <https://doi.org/10.4319/lom.2014.12.10>
- Fenner, N., Freeman, C., & Reynolds, B. (2005). Hydrological effects on the diversity of phenolic degrading bacteria in a peatland: implications for carbon cycling. *Soil Biology and Biochemistry*, 37, 1277–1287. <https://doi.org/10.1016/j.soilbio.2004.11.024>
- Fenner, N., & Freeman, C. (2011). Drought-induced carbon loss in peatlands. *Nature Geoscience*, 4, 895–900. <https://doi.org/10.1038/ngeo1323>
- Fowler, D., Coyle, M., Skiba, U., Sutton, M. A., Cape, J. N., Reis, S., et al. (2013). The global nitrogen cycle in the twenty-first century. *Philosophical Transactions of the Royal Society B: Biological Sciences*, 368, 20130164. <https://doi.org/10.1098/rstb.2013.0164>
- Greenan, C. M., Moorman, T. B., Kaspar, T. C., Parkin, T. B., & Jaynes, D. B. (2006). Comparing Carbon Substrates for Denitrification of Subsurface Drainage Water. *Journal of Environmental Quality*, 35(3), 824–829. <https://doi.org/10.2134/jeq2005.0247>
- Greenan, C. M., Moorman, T. B., Parkin, T. B., Kaspar, T. C., & Jaynes, D. B. (2009). Denitrification in Wood Chip Bioreactors at Different Water Flows. *Journal of Environmental Quality*, 38(4), 1664–1671. <https://doi.org/10.2134/jeq2008.0413>
- Healy, M. G., Ibrahim, T. G., Lanigan, G. J., Serrenho, A. J., & Fenton, O. (2012). Nitrate removal rate, efficiency and pollution swapping potential of different organic carbon media in laboratory

denitrification bioreactors. *Ecological Engineering*, 40, 198–209.

<https://doi.org/10.1016/j.ecoleng.2011.12.010>

Jaynes, D. B., & Isenhardt, T. M. (2019). Performance of saturated riparian buffers in Iowa, USA. *Journal of Environmental Quality*, 48(2), 289–296. <https://doi.org/10.2134/jeq2018.03.0115>

Maxwell, B. M., Birgand, F., Schipper, L. A., Christianson, L. E., Tian, S., Helmers, M. J., Williams, D. J., Chescheir, G. M., & Youssef, M. A. (2019a). Drying–Rewetting Cycles Affect Nitrate Removal Rates in Woodchip Bioreactors. *Journal of Environmental Quality*, 48(1), 93–101.

<https://doi.org/10.2134/jeq2018.05.0199>

Maxwell, B. M., Birgand, F., Schipper, L. A., Christianson, L. E., Tian, S., Helmers, M. J., Williams, D. J., Chescheir, G. M., & Youssef, M. A. (2019b). Increased Duration of Drying–Rewetting Cycles Increases Nitrate Removal in Woodchip Bioreactors. *Agricultural & Environmental Letters*, 4(1), 190028.

<https://doi.org/10.2134/aer2019.07.0028>

Maxwell, B. M., Díaz-García, C., José Martínez-Sánchez, J., Birgand, F., & Álvarez-Rogel, J. (2020).

Temperature sensitivity of nitrate removal in woodchip bioreactors increases with woodchip age and following drying–rewetting cycles. *Environmental Science: Water Research & Technology*, 6(10),

2752–2765. <https://doi.org/10.1039/D0EW00507J>

McClain, M. E., Boyer, E. W., Lisa Dent, C., Gergel, S. E., Grimm, N. B., Groffman, P. M., et al. (2003).

Biogeochemical hot spots and hot moments at the interface of terrestrial and aquatic ecosystems.

Ecosystems, 6, 301–312. <https://doi.org/10.1007/s10021-003-0161-9>

McGuire, P. M., Dai, V., Walter, T. M., & Reid, M., C. (2021). Labile carbon release from oxic–anoxic cycling in woodchip bioreactors enhances nitrate removal without increasing nitrous oxide accumulation. *Environmental Science: Water Research & Technology*, 7(12), 2357–2371.

<https://doi.org/10.1039/D1EW00446H>

Miller, A. E., Schimel, J. P., Meixner, T., Sickman, J. O., & Melack, J. M. (2005). Episodic rewetting enhances carbon and nitrogen release from chaparral soils. *Soil Biology and Biochemistry*, 37(12), 2195–2204. <https://doi.org/10.1016/j.soilbio.2005.03.021>

National Research Council, et al. (2000). *Clean coastal waters: Understanding and reducing the effects of nutrient pollution*. Committee on the Causes and Management of Eutrophication, Ocean Studies Board, Water Science and Technology Board, Commission on Geosciences, Environment and Resources, Division on Earth and Life Studies, National Academies Press.
<https://doi.org/10.17226/9812>

Robertson, W. D. (2010). Nitrate removal rates in woodchip media of varying age. *Ecological Engineering*, 36(11), 1581–1587. <https://doi.org/10.1016/j.ecoleng.2010.01.008>

Robertson, W. D., Blowes, D. W., Ptacek, C. J., & Cherry, J. A. (2000). Long-term performance of in situ reactive barriers for nitrate remediation. *Ground Water*, 38(5), 689–695.

RStudio Team. (2020). *RStudio: Integrated Development for R*. RStudio, PBC. <https://www.rstudio.com/>

Saraswati, S., Dunn, C., Mitsch, W. J., & Freeman, C. (2016). Is peat accumulation in mangrove swamps influenced by the “enzymic latch” mechanism? *Wetlands Ecology and Management*, 24, 641-650.
<https://doi.org/10.1007/s11273-016-9493-z>

Schipper, L. A., Robertson, W. D., Gold, A. J., Jaynes, D. B., & Cameron, S. C. (2010). Denitrifying bioreactors—An approach for reducing nitrate loads to receiving waters. *Ecological Engineering*, 36(11), 1532–1543. <https://doi.org/10.1016/j.ecoleng.2010.04.008>

Van Cleemput, O., Boeckx, P., Lindgren, P.-E., & Tonderski, K. (2007). Chapter 23—Denitrification in Wetlands. In H. Bothe, S. J. Ferguson, & W. E. Newton (Eds.), *Biology of the Nitrogen Cycle* (pp. 359–367). Elsevier. <https://doi.org/10.1016/B978-044452857-5.50024-2>

Volokita, M., Belkin, S., Abeliovich, A., & Soares, M. I. M. (1996). Biological denitrification of drinking water using newspaper. *Water Research*, 30(4), 965–971. [https://doi.org/10.1016/0043-1354\(95\)00242-1](https://doi.org/10.1016/0043-1354(95)00242-1)

Zarnetske, J. P., Haggerty, R., Wondzell, S. M., & Baker, M. A. (2011). Labile dissolved organic carbon supply limits hyporheic denitrification. *Journal of Geophysical Research: Biogeosciences*, 116(G4).
<https://doi.org/10.1029/2011JG001730>